

One-loop corrections, uncertainties, and approximations in neutralino annihilations: ExamplesF. Boudjema,¹ G. Drieu La Rochelle,^{1,2} and S. Kulkarni³¹*LAPTh*, Université de Savoie, CNRS, B.P.110, Annecy-le-Vieux F-74941, France*²*CERN Physics Department, Theory Division, CH-1211 Geneva 23, Switzerland*³*Bethe Center for Theoretical Physics and Physikalisches Institut, Universität Bonn, Nussallee 12, D-53115 Bonn, Germany*

(Received 23 August 2011; published 8 December 2011)

The extracted value of the relic density has reached the few percent level precision. One can therefore no longer content oneself with calculations of this observable where the annihilation processes are computed at tree level, especially in supersymmetry where radiative corrections are usually large. Implementing full one-loop corrections to all annihilation processes that would be needed in a scan over parameters is a daunting task. On the other hand one may ask whether most of the corrections are taken into account through effective couplings of the neutralino that improve the tree-level calculation and would be easy to implement. We address this issue by concentrating in this first study on the neutralino coupling to (i) fermions and sfermions and (ii) Z . After constructing the effective couplings we compare their efficiency to the full one-loop calculation and comment on the failures and success of the approach. As a bonus we point out that large nondecoupling effects of heavy sfermions could in principle be measured in the annihilation process, a point of interest in view of the latest limit on the squark masses from the LHC. We also comment on the scheme dependencies of the one-loop corrected results.

DOI: [10.1103/PhysRevD.84.116001](https://doi.org/10.1103/PhysRevD.84.116001)

PACS numbers: 95.35.+d, 11.10.Gh, 11.30.Pb, 98.80.-k

I. INTRODUCTION

With barely 1 fb^{-1} of data, the LHC is pushing many hitherto popular, though naive, extensions of supersymmetry to the corners of high masses [1] while leaving some hope for a discovery of a rather light Higgs particle that could still be compatible with supersymmetry [2]. Before this very recent paradigm, supersymmetric models (and most models of new physics for that *matter*) were very strenuously constrained to a thin sliver in parameter space, most notably from the very precise measurement of the dark matter relic density that has now reached the few percent level and that will get even more precise in the future, hence cornering even further model building. Combining the results of the 7-year WMAP data [3] on the 6-parameter Λ CDM model, the baryon acoustic oscillations from SDSS [4] and the most recent determination of the Hubble constant [5] one [6] arrives at $\Omega_{\text{CDM}} h^2 = 0.1123 \pm 0.0035$, where Ω_{CDM} is the density of cold dark matter (CDM) normalized to the critical density, and h is the Hubble constant in units of $100 \text{ km s}^{-1} \text{ Mpc}^{-1}$. One has reached a precision of 3%. The data from the LHC do not infer that dark matter within supersymmetry, exemplified most nicely through the neutralino, the lightest supersymmetric particle (LSP), is of order of 1 TeV or so; this is just a limit on the colored constituents of the model. As for the Higgs particle, were it not for the large radiative corrections on the mass of the lightest member, supersymmetry would long be a forlorn construct. The Higgs particle is the most prominent example where radiative corrections are far from negligible in supersymmetry, yet

practically all analyses that aim at constraining the parameter space of the minimal supersymmetric standard model (MSSM) through the relic density are based on tree-level cross sections of the annihilation processes entering the predictions of this quantity which, as stressed, is experimentally given within the percent accuracy. Only seldom do some analyses assign a theory uncertainty to these annihilation cross sections, an uncertainty due essentially to the fact that higher order loop effects are not known. This uncertainty, in the rare case where it is taken into account, is however assumed to be invariably the same whatever the nature of the dominant process and the composition of the LSP. The reason the loop corrections are ignored, irrespective of the model specified, is that the calculation of the relic density requires most often the evaluation of a large number of processes. Most analyses are done with public codes [7–9] based on tree-level calculations. Computations of the relic density at one loop have now been achieved for quite a few channels [10–14] and tools exist now to perform in principle any calculation of the relic density beyond tree-level amplitudes thanks to the recent development of adapted automation tools [15]. Beside the findings [10–14] that these corrections are important, the improvements have not percolated into most analyses. It must be said that these calculations do involve some nontrivial issues about the renormalization of the MSSM and more generally techniques for one-loop integrals that certainly require expertise. The other reason is that even when they could be implemented, they are still certainly extremely CPU time consuming, forbidding any attempts of fits, likelihood search, and in a more general context any sampling of the parameter space, especially if one takes into account the fact that the MSSM is more than

*UMR 5108 du CNRS, associée à l'Université de Savoie.

liberal with unconstrained parameters. Yet, apart from providing a more precise prediction, one-loop calculations can probe higher masses, a situation akin to the precision electroweak observables and their sensitivity to the top and Higgs mass. For example, nondecoupling corrections have been revealed in one-loop calculations of supersymmetry observables [16–18]. They stem from the superoblique contribution which is termed in analogy to the more familiar oblique corrections that appear in one-loop corrections to 4-fermion processes in the standard model. They originate from the universal, process-independent self-energy corrections. An example in view of the recent findings of the LHC is that super heavy squarks leave a non-negligible imprint on many observables, in particular, the annihilation cross sections involving dark matter.

The aim of this paper is two-fold. First, to stress again the importance of the loop corrections for the relic density and show again that even when a loop calculation is available, there still remains in some cases an uncertainty that pertains to the choice of the renormalization scheme. The second and more detailed aspect is to discuss whether an approximation to the one-loop calculation can be found. We aim at implementing a universal correction through effective couplings of the LSP and checking its validity against a complete one-loop calculation. If such an approximation is possible and general enough, it could be implemented in existing codes (based on tree-level cross sections) calculating the relic density. Such was the case with the inclusion of the Sommerfeld effect [19] in the case of coannihilation or processes dominated by Higgs exchange for which Δm_b [20] corrections are included [7].

This preliminary study takes a simple process, namely $\tilde{\chi}_1^0 \tilde{\chi}_1^0 \rightarrow \mu^+ \mu^-$, as a testing ground. The aim of this study is not to find a good scenario that returns the correct actual value of the relic density but to try to unravel some general common features of the loop calculation to improve the predictions of the relic density. The aim is to rather find out whether one can improve on the tree-level calculation by introducing effective couplings of the LSP that could be used for any process. As we will see, though at first sight naive, the process $\tilde{\chi}_1^0 \tilde{\chi}_1^0 \rightarrow \mu^+ \mu^-$ embodies the three types of couplings of the neutralino: to f/\tilde{f} , gauge bosons, and Higgs particles. Here we cover the bino and the Higgsino

case. One might argue that the bino case corresponds to what was referred to as the bulk region in the constrained MSSM and is largely ruled out, whereas for a Higgsino this would not be the dominant process. As we have just stressed, the aim is not to strive to find a good scenario. Besides, it suffices to change the cosmological ingredients [21] entering the calculation of the relic density to revive the so-called bulk region. We will see that by considering these few simple examples the conclusions about the efficacy of the effective coupling is quite different. Moreover, there is no need here to convert a full corrected cross section into a relic density value; we rather take for all the models we study the annihilation cross section for an energy corresponding to a relative velocity of $v = 0.2$, typical for the relic density calculation. As known, for zero relative velocity the process enjoys chirality suppression which is lifted at higher order through gauge boson radiation; however the effect on the relic is totally marginal [10].

The paper is organized as follows. We first briefly describe the ingredients necessary to perform a one-loop calculation in supersymmetry covering both automation and renormalization schemes; it is in this section that we will write down the effective universal neutralino couplings as well as some definitions. Section III contains our main results. After a few definitions we first study the case of a binolike neutralino before addressing the case of a Higgsino-like LSP. We also quantify the possible uncertainties due to the scheme dependence. We conclude in Sec. IV by some general observations.

Throughout the paper we use some shorthand notation for angles. Generically c_θ , s_θ , t_θ stand for $\cos\theta$, $\sin\theta$, $\tan\theta$. The weak mixing angle θ_W is defined as $\cos\theta_W = c_W = M_W/M_Z$, where M_W is the W mass and M_Z the Z mass.

II. CALCULATIONS, RENORMALIZATION SCHEMES AT FULL ONE-LOOP

A. Tree-level considerations

At tree level (see Fig. 1), $\tilde{\chi}_1^0 \tilde{\chi}_1^0 \rightarrow \mu^+ \mu^-$ proceeds through (i) t -channel smuon exchange dominated by a $\tilde{\mu}_R$ in the case of a binolike since it has the largest hypercharge; (ii) a Z exchange which, on the other hand, is

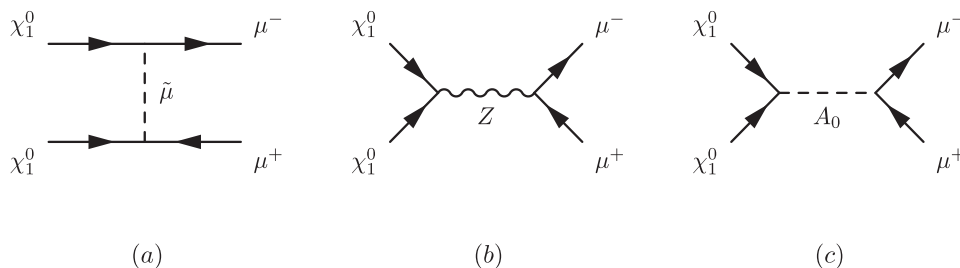


FIG. 1. Tree-level diagrams contributing to $\tilde{\chi}_1^0 \tilde{\chi}_1^0 \rightarrow \mu^+ \mu^-$. (a) is the t -channel $\tilde{\mu}$ exchange, (b) is the Z exchange, and (c) an example of a Higgs exchange.

suppressed for the bino; and (iii) Higgs exchange, but this is small in view of the Yukawa coupling of the muon. Therefore, as advertised, all types of couplings for the LSP are present: to fermions in the $\tilde{\chi}_1^0 \tilde{\mu} \mu$ coupling, gauge bosons in the $\tilde{\chi}_1^0 \tilde{\chi}_1^0 Z$, and Higgs scalars such as $\tilde{\chi}_1^0 \tilde{\chi}_1^0 A^0$ (A^0 is the pseudoscalar Higgs). It is through the choice of a hierarchy in the set M_1, M_2, μ that we can largely define the nature of the LSP. Numerically speaking we call a neutralino pure or almost pure when its mixing to the specified species is over 99%.

B. Renormalization and loop corrections, general considerations and issues

1. Set up of the automatic calculation: SLOOPS

One-loop processes calculated via the diagrammatic Feynman approach involve a huge number of diagrams even for $2 \rightarrow 2$ reactions, especially in a theory like supersymmetry. Performing a full one-loop calculation by hand without automation is practically untractable. Our exact full one-loop calculation is done with the help of the automated code SLOOPS. SLOOPS is an automated code for one-loop calculations in supersymmetry. It is a combination of LANHEP [22], the bundle FEYNARTS [23], FORMCALC [24], and an adapted version of LOOPTOOLS [25,26]. LANHEP deals with one of the main difficulties that has to be tackled for the automation of the implementation of the model file, which is entering the thousands of vertices that define the Feynman rules. On the theory side, a proper renormalization scheme needs to be set up, which then means extending many of these rules to include counterterms. This part is done through LANHEP which allows one to shift fields and parameters and thus generate counterterms most efficiently. The ghost Lagrangian is derived directly from the Becchi-Rouet-Stora-Tyutin charge (BRST) transformations. The loop libraries used in SLOOPS are based on LOOPTOOLS with the addition of quite a few routines, in particular, those for dealing with small Gram determinants that appear in our case at small relative velocities of the annihilating dark matter, and even more so of relevance for indirect detection [26].

2. Renormalization

In SLOOPS all sectors of the MSSM are implemented through a one-loop renormalization. This is explained in detail in [10,13,27,28]. Here we only briefly sketch the renormalization procedure. We have worked, as far as possible, within an on-shell scheme generalizing what is done for the electroweak standard model [29].

(i) The standard model (SM) parameters: the fermion masses as well as the mass of the W and Z are taken as input physical parameters. The electric charge is defined in the Thomson limit; see for example [29]. The light quarks (effective) masses are chosen [30] so as to reproduce the SM value of $\alpha^{-1}(M_Z^2) = 127.77$. This should be kept in

mind since one would be tempted to use a $\overline{\text{DR}}$ scheme for α , defined as M_Z , to take into account the fact that dark matter is annihilating at roughly the electroweak scale, so that $\alpha((2m_{\tilde{\chi}_1^0})^2)$ is a more appropriate choice. One should remember that the use of $\alpha((2m_{\tilde{\chi}_1^0})^2)$ instead of the on-shell value in the Thomson limit would correct the tree-level cross section for $\tilde{\chi}_1^0 \tilde{\chi}_1^0 \rightarrow \mu^+ \mu^-$ by about 14%, independently of the neutralino mass in the range $50 < M_{\tilde{\chi}_1^0} < 300$ GeV. As we will see and have reported elsewhere for other processes this running does not, most of the time, take into account the bulk of the radiative corrections that we report here. Therefore for further reference, let us introduce the correction due to the running of α ,

$$\Delta_\alpha = \frac{\sigma_{\text{eff}} - \sigma_0}{\sigma_0} = 2\Delta\alpha, \quad (1)$$

where the cross section σ_0 is the tree level calculated with $\alpha_0 = \alpha(0) = 1/137.0359895$, whereas σ_{eff} is the tree level with $\alpha_0 \rightarrow \alpha_{\text{eff}}(Q^2) = \alpha(Q^2) = \alpha_0/(1 + \Delta\alpha(Q^2))$, $Q = 2m_{\tilde{\chi}_1^0}$. With our input parameters $\Delta\alpha(M_Z^2) = 0.06$. In the running we allow for all charged particles including the W boson contribution, the top and the sfermions, and the charginos, though for the light LSP scenario we consider these added contributions are very small¹

(ii) The Higgs sector: the pseudoscalar Higgs mass M_A^0 is used as an input parameter while insisting on vanishing tadpoles. t_β , which at tree level is the ratio of the two expectation values of the Higgs doublets, can be defined through several schemes:

- (a) In the Dabelstein-Chankowski-Pokorski-Rosiek (DCPR) scheme [31,32] t_β is defined by requiring that the (renormalized) $A^0 Z$ transition vanishes at $Q^2 = M_{A^0}^2$.
- (b) A $\overline{\text{DR}}$ definition where the t_β counter term, δt_β , is defined as a pure divergence leaving out all finite parts.
- (c) A process-dependent definition of this counterterm by extracting it from the decay $A^0 \rightarrow \tau^+ \tau^-$ that we will refer to as $A_{\tau\tau}$ for short. This definition is a good choice for the gauge independence of the processes.
- (d) An on-shell definition with the help of the mass of the heavy CP Higgs H taken as input parameter called the MH scheme from now on. We have reported elsewhere that this scheme usually introduces large radiative corrections.

These schemes are critically reviewed in [27]. By default we use the DCPR scheme but when quantifying the effect of the scheme dependence on t_β we also use the $\overline{\text{DR}}$ and MH scheme.

¹For the W boson contribution the self-energy of the photon is calculated in a nonlinear gauge [29] corresponding to the background gauge in order to maintain $U(1)_{\text{QED}}$ gauge invariance.

(iii) The sfermion sector: for the process at hand only the smuon parameters require renormalization. For the slepton sector we use as input parameters masses of the two charged sleptons which in the case of no-mixing define the R -slepton soft breaking mass, $M_{\tilde{\mu}_R}$ and the $SU(2)$ mass, $M_{\tilde{\mu}_L}$, giving a correction to the sneutrino mass at one loop. Though not needed here, in the squark sector each generation needs three physical masses to constrain the breaking parameter $M_{\tilde{Q}_L}$ for the $SU(2)$ part, $M_{\tilde{u}_R}$, $M_{\tilde{d}_R}$ for the R part. See [28] for details.

(iv) The chargino/neutralino sector: first of all, for the neutralinos at tree level the physical fields χ_i^0 , $i = 1, \dots, 4$ are obtained from the current eigenstates $(\psi^n)^t = (\tilde{B}^0, \tilde{W}^0, \tilde{H}_1^0, \tilde{H}_2^0)$ through a unitary complex matrix N

$$\chi^0 = N\psi^n. \quad (2)$$

N diagonalizes the mass mixing matrix Y in the neutralino sector; see [28] for details and conventions. Although only $\tilde{\chi}_1^0$ enters our calculations we do need to fix all the elements that define its composition and hence couplings. For this sector we implement an on-shell scheme by taking as input three masses in order to reconstruct the underlying parameters M_1 , M_2 , μ . In SLOOPS [28] the default scheme is to choose two chargino masses $m_{\tilde{\chi}_1^\pm}$ and $m_{\tilde{\chi}_2^\pm}$ as input to define M_2 and μ and one neutralino mass to fix M_1 . The masses of the remaining three neutralinos receive one-loop quantum corrections. In this scheme, these counterterms are [28]

$$\begin{aligned} \delta M_2 &= \frac{1}{M_2^2 - \mu^2} \left((M_2 m_{\tilde{\chi}_1^+}^2 - \mu \det X) \frac{\delta m_{\tilde{\chi}_1^+}}{m_{\tilde{\chi}_1^+}} + (M_2 m_{\tilde{\chi}_2^+}^2 - \mu \det X) \frac{\delta m_{\tilde{\chi}_2^+}}{m_{\tilde{\chi}_2^+}} - M_W^2 (M_2 + \mu s_{2\beta}) \frac{\delta M_W^2}{M_W^2} - \mu M_W^2 s_{2\beta} c_{2\beta} \frac{\delta t_\beta}{t_\beta} \right), \\ \delta \mu &= \frac{1}{\mu^2 - M_2^2} \left((\mu m_{\tilde{\chi}_1^+}^2 - M_2 \det X) \frac{\delta m_{\tilde{\chi}_1^+}}{m_{\tilde{\chi}_1^+}} + (\mu m_{\tilde{\chi}_2^+}^2 - M_2 \det X) \frac{\delta m_{\tilde{\chi}_2^+}}{m_{\tilde{\chi}_2^+}} - M_W^2 (\mu + M_2 s_{2\beta}) \frac{\delta M_W^2}{M_W^2} - M_2 M_W^2 s_{2\beta} c_{2\beta} \frac{\delta t_\beta}{t_\beta} \right), \end{aligned} \quad (3)$$

$$\delta M_1 = \frac{1}{N_{1i}^2} (\delta m_{\chi_i^0} - N_{2i}^2 \delta M_2 + 2N_{3i} N_{4i} \delta \mu - 2N_{1i} N_{3i} \delta Y_{13} - 2N_{2i} N_{3i} \delta Y_{23} - 2N_{1i} N_{4i} \delta Y_{14} - 2N_{2i} N_{4i} \delta Y_{24}), \quad (4)$$

with $\det X = M_2 \mu - M_W^2 s_{2\beta}$ [28]. $\delta m_{\chi_i^0}$ is the counterterm of i th neutralino defined entirely from its self-energy; see [28]. δO represents the shift on the parameter O that generates the counterterm for that quantity. Looking at these equations some remarks can be made. First, in the special configuration $M_2 \sim \pm \mu$ an apparent singularity might arise. Reference [10] pinpointed this configuration which can induce a large t_β -scheme dependence in the counterterms $\delta M_{1,2}$ and $\delta \mu$. Such a mixed scenario is not covered here. Second, the choice of $m_{\tilde{\chi}_1^0}$ as an input parameter is appropriate only if the lightest neutralino is mostly bino ($|N_{11}| \sim 1$) or if the binolike neutralino is not too heavy compared to other neutralinos. Indeed we can see that if $N_{1i} \sim 0$ the counterterm δM_1 is subject to large uncertainty and may introduce a large finite correction; this is related to the fact that M_1 is badly reconstructed. To avoid such uncertainty we only choose i as the most binolike; in other words in Eq. (4), $|N_{1i}| = \text{Max}(|N_{1j}|)$, $j = 1, \dots, 4$.

v) Finally diagonal field renormalization is fixed by demanding the residue at the pole of the propagator of all physical particles to be unity, and the nondiagonal part by demanding no mixing between the different physical particles when on shell. This is implemented in all the sectors. In our case apart from the muon, this step is important for the $\tilde{\chi}_1^0$. We insist that N_{ij} is used both at the tree level and one-loop level. Nonetheless to define the physical state we do introduce the shift for the neutralinos [28] through wave function renormalization

$$\tilde{\chi}_i^0 \rightarrow \tilde{\chi}_i^0 + \frac{1}{2} \sum_j (\delta Z_{ij} P_L + \delta Z_{ij}^* P_R) \tilde{\chi}_j^0. \quad (5)$$

(vi) Dimensional reduction is used as implemented in the FEYNARTS-FORMCALC-LOOPTOOLS bundle at one-loop through the equivalent constrained dimensional renormalization [33].

3. Infrared divergences

For the processes $\tilde{\chi}_1^0 \tilde{\chi}_1^0 \rightarrow \mu^+ \mu^-$, we can decompose the one-loop amplitudes in a virtual part $\mathcal{M}_{1\text{loop}}^{\text{EW}}$ and a counterterm (CT) contribution \mathcal{M}_{CT} . The sum of these two amplitudes must be ultraviolet finite and gauge independent. Because of the virtual exchange of the massless photon, this sum can contain infrared divergencies. This is cured by adding a small mass to the photon and/or gluon, λ_γ and λ_g . This mass regulator should exactly cancel against the one present in the final-state radiation of a photon. The QED contribution is therefore split into two parts: a soft one where the photon energy E_γ is integrated to less than some small cutoff k_c and a hard part with $E_\gamma > k_c$. The former requires a photon mass regulator. Finally the sum $\mathcal{M}_{1\text{loop}} + \mathcal{M}_{\text{CT}} + \mathcal{M}_\gamma^{\text{soft}}(E_\gamma < k_c) + \mathcal{M}_{\gamma,g}^{\text{hard}}(E_{\gamma,g} > k_c)$ should be ultraviolet finite, gauge invariant, not depend on the mass regulator, and on the cut k_c .

4. Checking the result

(i) For each process and set of parameters, we first check the ultraviolet finiteness of the results. This test applies to the whole set of virtual one-loop diagrams. The ultraviolet finiteness test is performed by varying the ultraviolet parameter $C_{UV} = 1/\varepsilon$, ε is the usual regulator in dimensional reduction. We vary C_{UV} by 7 orders of magnitude with no change in the result. We content ourselves with double precision.

(ii) The test on the infrared finiteness is performed by including both the loop and the soft bremsstrahlung contributions and checking that there is no dependence on the fictitious photon mass λ_γ .

(iii) Gauge parameter independence of the results is essential. It is performed through a set of the *eight* gauge fixing parameters based on the implementation of a non-linear gauge [27].

C. Effective couplings for neutralino interactions vs full calculation

1. Contributions at full one loop

The full set of one-loop contributions to the process $\tilde{\chi}_1^0 \tilde{\chi}_1^0 \rightarrow \mu^+ \mu^-$ consists of two-point functions (self-energies and transitions such as $\tilde{\chi}_1^0 \rightarrow \tilde{\chi}_2^0$), vertex three-point functions as in Figs. 2(a) and 2(b), and box diagrams. The vertex corrections include also the counterterms; the latter as explained previously involve two-point functions. To these, one should also add the QED final-state radiation.

2. Effective couplings of the neutralino at one loop

Among this full set of corrections one can construct a finite subset that is not specific to the muon. This subset will be involved in all processes involving neutralinos. For example, the vertex correction to $\tilde{\chi}_1^0 \tilde{\chi}_1^0 Z$ is obviously independent of the muon being in the final state; a similar statement can be said for $\tilde{\chi}_1^0 \tilde{\chi}_1^0 h/H/A$. Also, all occurrences of the wave function renormalization of the neutralino (including transitions between neutralinos) and the Z are process independent. The same can be said also of the counterterms to the gauge couplings and the vacuum expectation values or in other words v , t_β . On the other hand the wave function

renormalization of the muon is specific to the muon final state. The boxes the four-point one-particle irreducible (1-PI) functions, as well as the QED correction are also specific to the process. The construct of the universal correction for the effective coupling $\tilde{\chi}_1^0 f \tilde{f}$ from $\tilde{\chi}_1^0 \mu \tilde{\mu}$ is different from that of $\tilde{\chi}_1^0 \tilde{\chi}_1^0 Z$, since in the latter all three particles can be considered as universal. For example the full correction to the vertex $\tilde{\chi}_1^0 \mu \tilde{\mu}$ shown in Fig. 2(a) consists of a 1-PI three-point function vertex correction (triangle) which is muon specific and that does not need to be calculated to build up the effective coupling. It also contains wave function renormalization of the neutralinos as well as counterterms for the gauge couplings and for other universal quantities such as t_β which must be combined to arrive at the universal correction for the $\tilde{\chi}_1^0 f \tilde{f}$ vertex. The aim of the paper is therefore to extract these process-independent contributions and define effective vertices for the LSP interactions. This is akin to the effective coupling of the Z to fermions where universal corrections are defined. Describing the bulk of the radiative corrections in terms of effective couplings has been quite successful to describe, for example, the observables at the Z peak. Although not describing most perfectly the effect of the full corrections for all observables (for example $Z b \bar{b}$ receives an important triangle contribution due to the large top Yukawa coupling) one must admit that the approach has done quite a good job. Most of the effective corrections were universal, described in terms of a small set of two-point functions of the gauge bosons.

The other benefit was that such approximations were sensitive to nondecoupling effects that probe higher scales (top mass and Higgs mass). The set of two-point functions, and for $\tilde{\chi}_1^0 \tilde{\chi}_1^0 Z$ three-point functions, should of course lead to a finite and gauge-invariant quantity. Loops involving gauge bosons have always been problematic (even in the case of the $Z f \tilde{f}$) in such an approach since it is difficult to extract a gauge-independent value. For the couplings of the neutralinos as would be needed for approximating their annihilation cross section independently of the final state, one would therefore expect that apart from the rescaling of the gauge couplings which can be considered as an overall constant, the mixing effect between the different neutralinos should be affected. One can in fact reorganize a

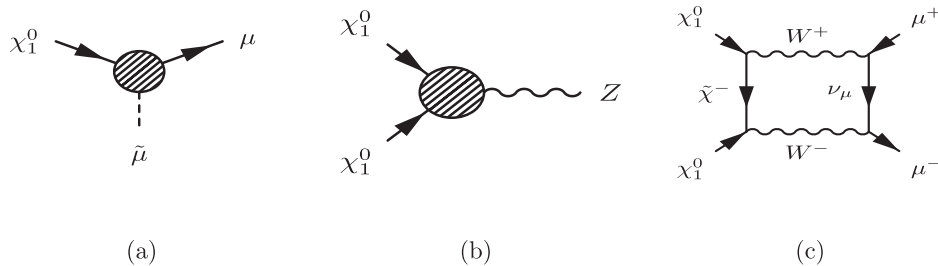


FIG. 2. Different types of corrections appearing at one-loop for the process $\tilde{\chi}_1^0 \tilde{\chi}_1^0 \rightarrow \mu^+ \mu^-$. (a) is the correction to vertex $\tilde{\chi}_1^0 \mu \tilde{\mu}$ for the t -channel $\tilde{\mu}$ exchange, (b) is the full correction to the $\tilde{\chi}_1^0 \tilde{\chi}_1^0 Z$ vertex for the s -channel Z exchange, and (c) is an example of a box loop.

few of the two-point functions (that can be written also as counterterms) to define an effective coupling for the neutralino. One should of course also correct in this manner the $Z\mu^+\mu^-$ coupling. Let us stress again that in this first investigation we will primarily take into account the effects of fermions and sfermions in the universal loops. For the $\tilde{\chi}_1^0\tilde{\chi}_1^0Z$ effective coupling we also attempt to include the virtual contribution of the gauge bosons especially since for the Higgsino-like case the couplings to W and Z are not suppressed.

3. The effective $\tilde{\chi}_1^0 f \tilde{f}$

To find the process-independent corrections to this coupling, we recall that in the basis $(\tilde{B}^0, \tilde{W}^0, \tilde{H}_1^0, \tilde{H}_2^0)$ before mixing and for both $f_{L,R}$ the couplings for the two chiral Lorentz structures write as

$$\begin{aligned} \frac{1}{\sqrt{2}}(g'Y_f, g\tau_f^3, y_{1,f}, y_{2,f}) &= \frac{1}{\sqrt{2}}\left(g'Y_f, g\tau_f^3, \frac{gm_u}{M_W c_\beta}, \frac{gm_d}{M_W s_\beta}\right) \\ &\rightarrow \left(g', g, \frac{g}{M_W c_\beta}, \frac{g}{M_W s_\beta}\right). \end{aligned} \quad (6)$$

Y_f, τ_f^3 are the isospin and $SU(2)$ charges of the corresponding fermion/sfermions. The two Higgsinos couple differently to the up and down fermions with a coupling that is proportional to the Yukawa coupling. Though this is not universal we can still isolate a universal part where there is no reference to the final fermion/sfermion. This is what is meant by the last expression in Eq. (6), where the explicit mass of the corresponding fermion masses has been dropped. The variations/counterterms on these parameters have to be implemented before turning to the physical basis. The latter as explained in the previous paragraph is achieved through the diagonalizing matrix N [Eq. (2)] as in tree-level supplemented by wave function renormalization which involve both diagonal and nondiagonal transitions of the neutralino; see Eq. (5). In the case of effective coupling of neutralinos, this is achieved by defining an effective mixing matrix such that $N \rightarrow N + \Delta N^{\chi f \tilde{f}}$ in all couplings of the neutralino. The $\Delta N^{\chi f \tilde{f}}$ write as

$$\begin{aligned} \Delta N_{i1}^{\chi f \tilde{f}} &= \frac{\delta g'}{g'} N_{i1} + \frac{1}{2} \sum_j N_{j1} \delta Z_{ji}, \\ \Delta N_{i2}^{\chi f \tilde{f}} &= \frac{\delta g}{g} N_{i2} + \frac{1}{2} \sum_j N_{j2} \delta Z_{ji}, \\ \Delta N_{i3}^{\chi f \tilde{f}} &= \left(\frac{\delta g}{g} - \frac{1}{2} \frac{\delta M_W^2}{M_W^2} - \frac{\delta c_\beta}{c_\beta}\right) N_{i3} + \frac{1}{2} \sum_j N_{j3} \delta Z_{ji}, \\ \Delta N_{i4}^{\chi f \tilde{f}} &= \left(\frac{\delta g}{g} - \frac{1}{2} \frac{\delta M_W^2}{M_W^2} - \frac{\delta s_\beta}{s_\beta}\right) N_{i4} + \frac{1}{2} \sum_j N_{j4} \delta Z_{ji}, \end{aligned} \quad (7)$$

where j runs from 1 to 4 and for the LSP, $i = 1$.

All the counterterms above are calculated from self-energy two-point functions and are fully defined in

[27,28]. $\delta g/g = \delta e/e - \delta s_W/s_W$, $\delta g'/g' = \delta e/e - \delta c_W/c_W$, and $\delta s_\beta/s_\beta = c_\beta^2 \delta t_\beta/t_\beta$. Equation (7) agrees with what was suggested in [34]. Let us stress again that in these self-energies no gauge bosons and therefore no neutralinos and charginos are taken into account but just sfermions and fermions; otherwise this would not be finite. For binolike case, self-energies containing gauge and Higgs bosons (with their supersymmetric counterparts) are not expected to contribute much. This is not necessarily the case for winos and Higgsinos.

4. The effective $\tilde{\chi}_1^0 \tilde{\chi}_1^0 Z$

Since all particles making this vertex can now be considered as being process independent (as far as neutralino annihilations are concerned), all counterterms including wave function renormalization of both the Z and $\tilde{\chi}_1^0$ must be considered. The price to pay now is that the genuine triangle vertex corrections $\tilde{\chi}_1^0 \tilde{\chi}_1^0 Z$ must also be included. It is only the sum of the vertex and the self-energies that renders a finite result. When correcting this vertex one must also correct the $Z\mu^+\mu^-$ vertex keeping within the spirit of calculating the universal corrections. This can be implemented solely through self-energy corrections (excluding the muon self-energies) and there is no need to calculate here the genuine vertex corrections. An exception would be the production of the b and to some extent the top quark where genuine vertex corrections are important. Talking of heavy flavors, when computing the correction to the $\tilde{\chi}_1^0 \tilde{\chi}_1^0 Z$ with the Z off shell with an invariant mass Q^2 , one should also include the $\tilde{\chi}_1^0 \tilde{\chi}_1^0 G^0$ vertex, where G^0 is the neutral Goldstone boson. In our case we restrict ourselves to almost massless fermions. The case of the top and bottom final states will be addressed elsewhere together with the potential relevant contribution of the Higgs particles in the s -channel.

Since one is including the genuine 1-PI vertex correction, it is important to inquire whether this correction generates a new Lorentz structure beyond the one found at tree level. The contribution to the tree-level Lorentz structure is finite after adding the self-energies and the vertex. Any new Lorentz structure will on the other hand be finite on its own. General arguments based on the Majorana nature of the neutralinos backed by our numerical studies show that no new Lorentz structure is generated for neutralinos. First of all, at tree level one has only one structure

$$\begin{aligned} \mathcal{L}_{\tilde{\chi}_1^0 \tilde{\chi}_1^0 Z} &= \frac{g_Z}{4} (N_{13} N_{13} - N_{14} N_{14}) \tilde{\chi}_1^0 \gamma_\mu \gamma_5 \tilde{\chi}_1^0 Z^\mu, \\ g_Z &= \frac{e}{c_W s_W}. \end{aligned} \quad (8)$$

The overall strength is a consequence of the fact that the coupling emerges solely from the Higgsino with a gauge coupling. Indeed in the $(\tilde{B}^0, \tilde{W}^0, \tilde{H}_1^0, \tilde{H}_2^0)$ basis the coupling is $\propto g_Z(0, 0, 1, -1)$. Only the Lorentz structure $\gamma_\mu \gamma_5$

survives as a consequence of the Majorana nature. With p_1, p_2 denoting the incoming momenta of the two $\tilde{\chi}_1^0$, at one-loop a contribution $(p_1^\mu - p_2^\mu)$ does not survive symmetrization, whereas $(p_1^\mu + p_2^\mu)$ will not contribute for massless muons. We calculate this correction for a Z with an invariant mass Q^2 ; in the application this Q^2 will be set to the invariant mass of the muon pair. This vertex contribution is denoted $\Delta g_{\tilde{\chi}_1^0 \tilde{\chi}_1^0 Z}^\Delta(Q^2) \equiv \Delta g_{\tilde{\chi}_1^0 \tilde{\chi}_1^0 Z}^\Delta$. The contribution of the coupling counterterms defining g_Z and the Z wave function renormalization define the universal correction to the Z coupling strength $g_Z^{\text{eff}} = g_Z(1 + \Delta g_Z)$, with $\Delta g_Z/g_Z = \delta g_Z/g_Z + \delta Z_{ZZ}/2$. δZ_{ZZ} is the wave function renormalization of the Z . We of course have to add the wave function renormalization of the $\tilde{\chi}_1^0$ like what was done for the $\tilde{\chi}_1^0 f \bar{f}$ vertex. We improve on this implementation by taking into account the fact that the Z is off shell and therefore the wave function renormalization through $\delta Z_{ZZ} = \Pi'_{ZZ}(M_Z^2)$ is only part of the correction that would emerge from the correction to the complete Z propagator in the s -channel contribution with invariant mass Q^2 . Note that here there is no need for including a $Z\gamma$ transition since photons do not couple to neutralinos. Collecting all these contributions, the effective vertex is obtained by making $g_Z \rightarrow g_{\tilde{\chi}_1^0 \tilde{\chi}_1^0 Z}^{\text{eff}}$ and $N_{i1} \rightarrow N_{i1} + \Delta N_{i1}^{\tilde{\chi}_1^0 \tilde{\chi}_1^0 Z}$ with

$$g_{\tilde{\chi}_1^0 \tilde{\chi}_1^0 Z}^{\text{eff}} = g_Z(1 + \Delta g_Z(Q^2) + \Delta g_{\tilde{\chi}_1^0 \tilde{\chi}_1^0 Z}^\Delta(Q^2)), \quad (9)$$

$$\Delta N_{ij}^{\tilde{\chi}_1^0 \tilde{\chi}_1^0 Z} = \frac{1}{2} \sum_k N_{kj} \delta Z_{ki}, \quad (i, j, k) = 1 \dots 4. \quad (10)$$

Explicitly

$$\begin{aligned} \Delta g_Z &= \frac{1}{2} \left(\Pi'_{\gamma\gamma}(0) - 2 \frac{s_W}{c_W} \frac{\Pi_{\gamma Z}(0)}{M_Z^2} \right) \\ &+ \frac{1}{2} \left(1 - \frac{c_W^2}{s_W^2} \right) \left(\frac{\Pi_{ZZ}(M_Z^2)}{M_Z^2} - \frac{\Pi_{WW}(M_W^2)}{M_W^2} \right) \\ &- \frac{1}{2} \left(\frac{\Pi_{ZZ}(Q^2) - \Pi_{ZZ}(M_Z^2)}{Q^2 - M_Z^2} \right). \end{aligned} \quad (11)$$

At the same time for the fermion with charge q_f we correct the $Z f \bar{f} \propto g_Z(\gamma_5 + (1 - 4|q_f|s_W^2))\gamma_\mu$ by effectively making $g_Z \rightarrow g_Z(1 + \Delta g_Z)$ with Δg_Z defined in Eq. (11) and s_W^2 to

$$\Delta s_W^2 = \frac{c_W^2}{s_W^2} \left(\frac{\Pi_{ZZ}(M_Z^2)}{M_Z^2} - \frac{\Pi_{WW}(M_W^2)}{M_W^2} \right) + \frac{c_W}{s_W} \frac{\Pi_{\gamma Z}(k^2)}{k^2}. \quad (12)$$

By default we include only the fermions and sfermions in the virtual corrections described by Eqs. (11) and (12). For the $\tilde{\chi}_1^0 \tilde{\chi}_1^0 Z$ one expects the contribution of the gauge bosons and the neutralinos/charginos to be non-negligible especially for the Higgsino case. In fact, including such contributions still gives an ultraviolet finite result for $g_{\tilde{\chi}_1^0 \tilde{\chi}_1^0 Z}^{\text{eff}}$ in

Eq. (11) which is a nontrivial result. Moreover this contribution is gauge parameter independent in the class of (linear) and nonlinear gauge fixing conditions [29]. To weigh up the gauge/gaugino/Higgsino contribution, we will therefore also compare with this generalized effective $g_{\tilde{\chi}_1^0 \tilde{\chi}_1^0 Z}^{\text{eff}}$ including all virtual particles. Observe that in Eq. (11) we have the contribution $\Pi_{\gamma Z}(0)$ which vanishes for fermions and sfermions but which is essential for the contribution of the virtual W . In any case, including gauge bosons in the renormalization of electromagnetic coupling requires the inclusion of the $\Pi_{\gamma Z}(0)$ in Eq. (11) for gauge invariance to be maintained [29]. We stress that we will present the effect of the generalized effective coupling $g_{\tilde{\chi}_1^0 \tilde{\chi}_1^0 Z}^{\text{eff}}$ as an indication of the gauge boson contribution while keeping in mind that this result may lead to unitarity violation. Indeed, through cutting rules, the W loop can be seen as made up of the scattering $W^+ W^- \rightarrow Z \rightarrow \mu^+ \mu^-$ that needs a compensation from the cut in the box shown in Fig. 2(c). For the effective $Z\mu^+\mu^-$ coupling we only include the fermion/sfermion contribution in Eqs. (11) and (12); adding the gauge bosons would require part of the 1-PI triangle contribution to $Z \rightarrow \mu^+ \mu^-$.

III. ANALYSIS

Since we will be studying different compositions of the neutralinos we will take different values for the set M_1, M_2, μ . On the other hand, the default parameters in the Higgs sector are

$$M_{A^0} = 1 \text{ TeV} \quad t_\beta = 4. \quad (13)$$

The sfermion sector is specified by a rather heavy spectrum (in particular within the limits set by the LHC for squarks [1]). All sleptons left and right of all generations have a common mass which we take to be different from the common mass in the squark sector. All trilinear parameters A_f (including those for stops and sbottom) are set to 0. The default values for the sfermion masses are

$$\begin{aligned} M_{\tilde{l}_R} &= M_{\tilde{l}_L} = 500 \text{ GeV}, \\ M_{\tilde{u}_R} &= M_{\tilde{d}_R} = M_{\tilde{Q}_L} = 800 \text{ GeV}, \\ A_f &= 0. \end{aligned} \quad (14)$$

By default we will focus on relatively light neutralinos (around 100 GeV) scattering with a relative velocity $v = 0.2$.

To analyze consistently the efficiency of effective corrections we will refer to the following quantities:

$$\Delta_{\text{eff}} = \frac{\sigma_{\text{eff}} - \sigma_0}{\sigma_0}. \quad (15)$$

Here σ_{eff} is the cross section calculated with the effective couplings that include, by default, universal process-independent particles excluding gauge bosons and gauginos/Higgsinos. We will explicitly specify when including

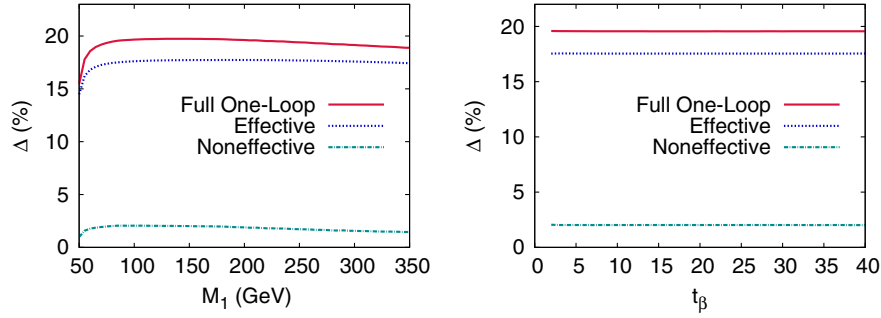


FIG. 3 (color online). Corrections to the tree-level cross section for the process $\tilde{\chi}_1^0 \tilde{\chi}_1^0 \rightarrow \mu^+ \mu^-$ in the bino case as a function of M_1 (left panel) and t_β (right panel). We show the full one-loop, the effective correction, and the difference which we term noneffective. $M_2 = 500$, $\mu = -600$ GeV.

all virtual particles in those corrections, referring to it as Δ_{eff}^W . This correction will be compared to the correction solely due to the running of the electromagnetic coupling; see Eq. (1). To see how well the correction through the effective couplings $\tilde{\chi}_1^0 f \tilde{f}$ and $\tilde{\chi}_1^0 \tilde{\chi}_1^0 Z$ reproduces the full one-loop correction we introduce

$$\Delta_{\text{NE}} = \frac{\sigma_{\text{one-loop}} - \sigma_{\text{eff}}}{\sigma_0}, \quad \Delta_{\text{full}} = \frac{\sigma_{\text{one-loop}} - \sigma_0}{\sigma_0}, \quad (16)$$

with $\sigma_{\text{one-loop}}$ the full one-loop cross section, Δ_{NE} measures what we will refer to as the noneffective (NE) corrections since this measures the remainder of all the corrections that are not taken into account by the effective vertices approach. $\Delta_{\text{full}} = \Delta_{\text{eff}} + \Delta_{\text{NE}}$ is the full one-loop correction.

A. Bino case

1. Effective vs full corrections

We first take $(M_1, M_2, \mu) = (90, 200, -600)$ GeV, which yields a lightest binolike neutralino (the bino composition is 99%) with mass $m_{\tilde{\chi}_1^0} = 91$ GeV. At tree level the cross section for relative velocity $v = 0.2$ is $\sigma_{\mu^+ \mu^-}^{\tilde{\chi}_1^0} = 6.75 \times 10^{-3}$ pb. Note for further reference that this is an order of magnitude larger than annihilation into a pair of W 's: $\sigma_{W^+ W^-}^{\tilde{\chi}_1^0} = 4.51 \times 10^{-4}$ pb. The annihilation proceeds predominantly through the t -channel; bino coupling to Z are very much reduced. This leads to the following set of corrections:

$$\begin{aligned} \Delta_{\text{eff}} &= 17.52\% (\Delta_\alpha = 14.56\%) \\ \Delta_{\text{NE}} &= 2.06\% (\Delta_{\text{full}} = 19.58\%). \end{aligned} \quad (17)$$

For our first try, the effective universal coupling does remarkably well, falling short of only 2% correction compared to the full calculation. Note that although the most naive implementation through a running of the electromagnetic coupling fares also quite well it is nonetheless 5% off the total correction, therefore the effective correction through the effective couplings performs better. It must

be admitted though that the bulk of the correction is through the running of α . To see how general this conclusion is we scanned over the set (M_1, M_2, μ) while maintaining $\tilde{\chi}_1^0$ with a 99% binolike component. This is simply obtained by taking $M_2 = 500$, $\mu = -600$ GeV, and scanning up to $M_1 = 350$ GeV. We also checked how sensitive our conclusion is depending on t_β by varying t_β from 2 to 40. The supersymmetry-breaking sfermion masses were first left to their default values. As Fig. 3 shows, our conclusions remain quantitatively unchanged. There is no appreciable dependence in t_β , we arrive at the same numbers as our default t_β value. As for the dependence in M_1 , it is very slight; for $M_1 \sim 50$ GeV there is perfect matching with our effective coupling implementation, then as M_1 increases to 350 GeV, the nonuniversal corrections remain negligible, below 2%.

The annihilation of neutralinos and hence the relic density is a very good example of the nondecoupling effects of very heavy sparticles, a remnant of supersymmetry breaking. The variation in the fermion/sfermion masses is all contained in the effective couplings that we have introduced. Leaving the dependence on the smuon mass at tree level, and the very small (see below) contribution of the smuon to the 1-PI vertex $\tilde{\chi}_1^0 \mu \tilde{\mu}$, the bulk of the smuon mass dependence is within the effective coupling. Figure 4

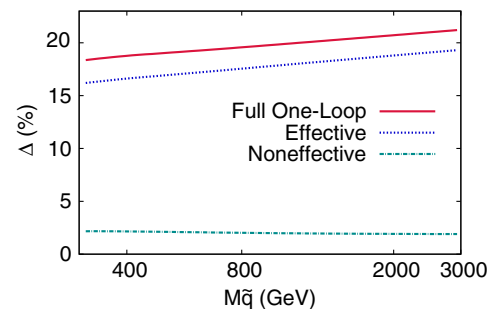


FIG. 4 (color online). Corrections to the tree-level cross section for the process $\tilde{\chi}_1^0 \tilde{\chi}_1^0 \rightarrow \mu^+ \mu^-$ in the bino case ($M_1 = 90$, $M_2 = 200$, $\mu = -600$ GeV) as a function of the common soft supersymmetry-breaking squark mass.

TABLE I. Coefficients of the $\ln(m_f)$ (running couplings) $\ln(m_{\tilde{f}})$ (nondecoupling effects) in Δ_{eff} . (c, s) give very similar results to (u, d) .

	$a_{\tilde{Q}_L}$	$a_{\tilde{u}_R}$	$a_{\tilde{d}_R}$	a_f	a_f
e	0.0010		0.002 31	0.003 10	0.15%
(u, d)	0.000 575	0.002 36	0.000 698	(0.004 13, 0.001 03)	0.15%
(t, b)	-0.004 06	0.008 38	0.000 661	(0.004 13, 0.001 03)	0.15%

shows how the correction increases as the mass of the squarks increases from 400 GeV to 3 TeV; we take here a common mass for the supersymmetry-breaking squark masses (both right and left in all three generations). The nonuniversal correction of about 2% is insensitive to this change in squark masses whereas both Δ_{eff} and Δ_{NE} show the same logarithm growth that brings a 3% change as the squark mass is varied in the range 400 GeV to 3 TeV. This result also confirms that genuine vertex corrections and box corrections are very small. We have also extracted the individual contribution of each species of fermions to the total nondecoupling effect of sfermions. To achieve this we numerically extracted the logarithm dependence of the nondecoupling effect for each species of sfermions. We have parametrized the effective correction as

$$\Delta^f = a_{\tilde{f}} \ln m_{\tilde{f}}/Q - a_f \ln m_f/Q + b_f \quad \text{with} \quad (18)$$

$$Q = 2m_{\tilde{\chi}_1^0} \quad \tilde{f} = \tilde{d}_R + \tilde{u}_R + \tilde{Q}_L.$$

The coefficients of the fit are given in Table I. As expected the fit to a_f is extremely well reproduced by the running of α , i.e., $a_f = N_c q_f^2 \frac{4\alpha}{3\pi}$. We also find $a_{\tilde{e}} = a_{\tilde{\tau}} = a_{\tilde{\mu}} = b_e = b_{\mu} = b_{\tau}$. The fit to a_f is made to validate the fit procedure. The most important observation is that the stops behave differently; this is due to the Yukawa coupling of the top and mixing. If there were not a compensation between the left and right contribution of the stops (compare to \tilde{u}) the contribution of the stops would be even more important and would dominate. Considering the different contributions and the scales that enter our calculations, it is difficult to attempt giving an analytical result. Leaving the stop aside, the different contributions to $a_{\tilde{f}}$ can be roughly approximated by $y_f^2 N_c N_d / 8 / c_W^2$, $N_d = 2$ for doublets and 1 for a singlet of $SU(2)$. y_f is the hypercharge, corresponding to the couplings of the sfermions to the bino component.

2. Scheme dependence in the bino case

We have compared the full correction to an approximate effective implementation and observed that the approximation is quite good. However, even the full correction, being computed at one loop, is potentially dependent on the renormalization scheme chosen. As discussed earlier, we analyze the t_β scheme dependence and the M_1 scheme dependence. For t_β we obtain the following corrections:

$$19.58\%(\text{DCPR}), \quad 19.79\%(\overline{\text{DR}}), \quad 19.51\%(\text{MH}).$$

This confirms that the t_β scheme dependence is very negligible. For the bino case, it is natural to reconstruct M_1 from the LSP; nonetheless analyzing the M_1 scheme dependence one chooses another neutralino, say $\tilde{\chi}_2^0$, which in our example is winolike. This introduces more uncertainty or error since with this scheme the corrections attain 24.08%, more than 4% compared to the usual scheme.

B. Higgsino case

1. Effective versus full corrections

In the bino case our trial point had a neutralino of mass 91 GeV. We therefore take the point (600, 500, -100) which gives a LSP with $M_{\tilde{\chi}_1^0} = 95$ GeV with a 99% Higgsino content. The sfermion parameters are the default values. In the Higgsino case the cross section is dominated by the exchange of the Z in the s -channel, so the bulk of the corrections through the effective couplings will be through the effective $\tilde{\chi}_1^0 \tilde{\chi}_1^0 Z$. For further reference note that the tree-level cross section for annihilation into muons is $\sigma_{\mu^+ \mu^-}^{\tilde{h}} = 2.58 \times 10^{-3}$ pb, tiny and totally insignificant especially compared to annihilation into W , $\sigma_{W^+ W^-}^{\tilde{h}} = 18.83$ pb. This is an observation we will keep in mind. The one-loop corrections we find for $\sigma_{\mu^+ \mu^-}^{\tilde{h}}$ are

$$\text{(for } \mu = -100 \text{ GeV)}$$

$$\Delta_{\text{eff}} = 13.55\% (\Delta_\alpha = 14.62\%) \quad (19)$$

$$\Delta_{\text{NE}} = -21.09\% (\Delta_{\text{full}} = -7.54\%).$$

This result is in a quite striking contrast to the bino case. The effective coupling does not reproduce at all the full correction and is off by as much as 21%. It looks like, at least for this particular choice of parameters, that going through the trouble of implementing the effective $\tilde{\chi}_1^0 \tilde{\chi}_1^0 Z$ was in vain since this correction is, within a percent, reproduced by the naive running of α . As we will see, both of these conclusions depend much on the parameters of the Higgsino and even the squark masses. For example consider $\mu = -50$ GeV, leaving all other parameters the same. Of course this is a purely academic exercise, since in this case, the charginos with mass $m_{\tilde{\chi}_1^\pm} = 55$ GeV are ruled out by LEP data. Nonetheless, in this case

$$\begin{aligned}
 (\text{for } \mu = -50 \text{ GeV}) \quad \Delta_{\text{eff}} &= 10.7(\Delta_\alpha = 12\%) \\
 \Delta_{\text{NE}} &= -6.9\%(\Delta_{\text{full}} = 3.8\%).
 \end{aligned}
 \tag{20}$$

Had we included all particles in the effective vertex, we would get a correction $\Delta_{\text{eff}}^W = 4.4\%$, improving thus the agreement with the one-loop correction for this particular value of μ up to 0.6%. At the same time a correction in terms of a running of α will be off by more than 8%.

These two examples show that one cannot, in the Higgsino case, draw a general conclusion on the efficiency of the effective coupling as was done in the bino case. Let us therefore look at how the corrections change with μ , and therefore with the mass of the LSP, while maintaining its Higgsino nature. We have varied μ from -200 GeV to -40 GeV. Figure 5 shows that the full correction is extremely sensitive to the value of μ . For $\mu = -200$ GeV the full one-loop correction is as much as -42% , casting doubt on the loop expansion. The effective coupling corrections with only fermions/sfermions on the other hand is much smoother and positive, bringing about 10% correction. Including all particles in the effective $\tilde{\chi}_1^0 \tilde{\chi}_1^0 Z$ vertex brings in an almost constant reduction of about 6%. Therefore as the value of $|\mu|$ increases, the effective one-loop corrections in the case of the Higgsino cannot be trusted. The same figure shows that the behavior and the increase in the corrections are due essentially to the contribution of the boxes. Here the boxes mean the non-QED box (involving an exchange of a photon which is infrared divergent before including the real photon emission²). The large contribution of the boxes can be understood by looking at the box in Fig. 1(c). Indeed, as argued previously, cutting through the box reveals that it represents $\tilde{\chi}_1^0 \tilde{\chi}_1^0 \rightarrow W^+ W^-$ production that rescatter into $\mu^+ \mu^-$. Both these processes have very large cross sections compared to the tree-level $\tilde{\chi}_1^0 \tilde{\chi}_1^0 \rightarrow \mu^+ \mu^-$. Our conclusion is therefore that the effective vertex approximation is inadequate as soon as the channel $\tilde{\chi}_1^0 \tilde{\chi}_1^0 \rightarrow W^+ W^-$ opens up. When this occurs, in practical calculations of the relic density, the channel $\tilde{\chi}_1^0 \tilde{\chi}_1^0 \rightarrow \mu^+ \mu^-$ is irrelevant and must rather analyze the loop corrections to $\tilde{\chi}_1^0 \tilde{\chi}_1^0 \rightarrow W^+ W^-$. This process was studied in [10,13] and will be investigated further through an effective approximation in a forthcoming study. On the other hand, the dependence of the relative correction on t_β is quite modest even though there is certainly more dependence than in the bino case, especially at lower values of $\tan\beta$. This is shown in Fig. 6.

We now investigate the nondecoupling of very heavy squarks (and heavy sfermions in general). Since we are in a Higgsino scenario, we expect the Yukawa coupling of the fermions to play a more prominent role than what was observed in the bino case. This is well supported by

²The contribution of the QED box + real photon emission is only 0.1%

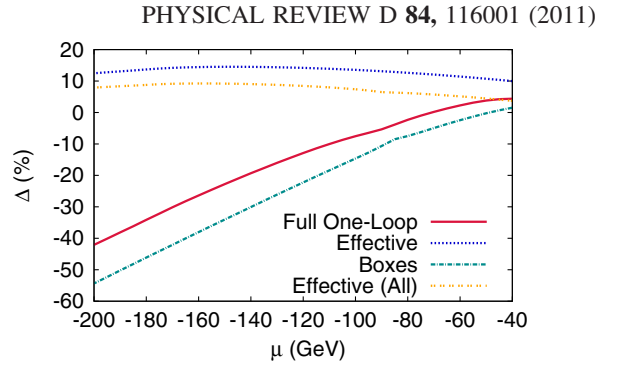


FIG. 5 (color online). Corrections to the tree-level cross section for the process $\tilde{\chi}_1^0 \tilde{\chi}_1^0 \rightarrow \mu^+ \mu^-$ in the Higgsino case as a function of μ . Shown are the effective vertex correction (Effective, with only fermions/sfermions in the loops), the effective $\tilde{\chi}_1^0 \tilde{\chi}_1^0 Z$ coupling including all particles [denoted Effective (All)], the non-QED boxes (Boxes), and the full correction. $M_2 = 500$, $M_1 = 600$ GeV.

our study. Figure 7 shows how the effective (with only fermions and sfermions) and the full correction get modified when the common mass of all squarks (all generations, left and right) increases from 400 GeV to 3 TeV. To better illustrate the important effect of the Yukawa coupling of the top/stop sector, we plot the corrections also for $m_t = 0.1$ GeV. For $m_t = 170.9$ GeV, the correction drops by about 13% when the mass of the squarks increases from 400 GeV to 3 TeV. This is much more dramatic than in the bino case where we observed a 3% increase in the same range. Observe that for our default squark mass of 800 GeV, the effective correction including sfermions/fermions is such that it almost accidentally coincides with the running of α . If one switches off the top quark mass, instead of a 13% decrease we observe an 8% increase for $m_t = 0.1$ GeV! Observe that the difference one sees for $m_{\tilde{Q}} = 400$ GeV between $m_t = 170.9$ GeV and $m_t = 0.1$ GeV is due essentially to the running of α with very light top that accounts for 3%.

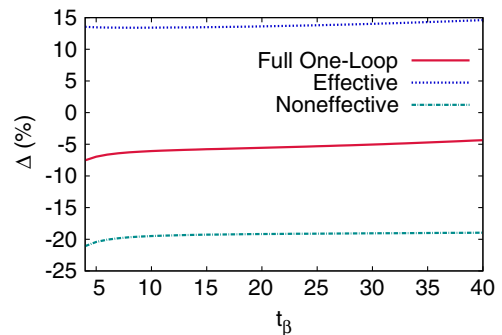


FIG. 6 (color online). Corrections to the tree-level cross section for the process $\tilde{\chi}_1^0 \tilde{\chi}_1^0 \rightarrow \mu^+ \mu^-$ in the Higgsino case as a function of t_β . We show the full one-loop, the effective correction, and the remainder (Noneffective). $\mu = -100$, $M_2 = 500$, $M_1 = -600$ GeV.

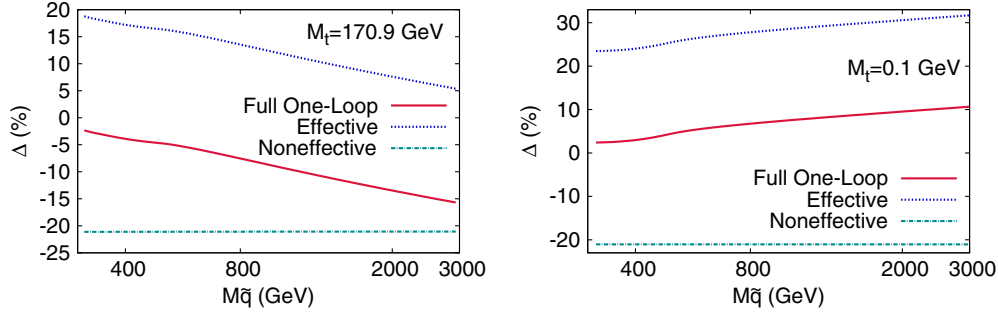


FIG. 7 (color online). Corrections to the tree-level cross section for the process $\tilde{\chi}_1^0\tilde{\chi}_1^0 \rightarrow \mu^+\mu^-$ in the Higgsino case ($M_1 = 600$, $M_2 = 500$, $\mu = -100$) as function of the common squark mass. The right panel illustrates the case $m_t = 0.1$ GeV.

The special role played by the top can be seen even more clearly from each individual contribution of the fermion/sfermions and the fit of the contribution according to Eq. (18) as was done for the bino case. The contribution of the stop is clearly (especially through \tilde{Q}_L) an order of magnitude larger than for all other sfermions; see Table II. It is the only one that brings a negative contribution. Since this effect is in the universal $\tilde{\chi}_1^0\tilde{\chi}_1^0Z$, it will show up in many processes where the Higgsino contributes.

2. Scheme dependence in the Higgsino case

We analyze here the t_β scheme dependence and the M_1 scheme dependence. For t_β we obtain the following corrections:

$$-7.5\%(\text{DCPR}), \quad -12.4\%(\overline{\text{DR}}), \quad -4.76\%(\text{MH}).$$

As expected and in line with the behavior of the corrections with respect to $\tan\beta$, Fig. 6, we see that the corrections though larger than in the bino case are nonetheless within 5%. On the other hand, as expected, the choice of M_1 has less impact than in the bino case, where the reconstruction of M_1 is essential to define the LSP. In the case of the Higgsino, changing the M_1 scheme turns the full correction from -7.5% (in DCPR scheme for t_β) to -10.7% , a 3% uncertainty.

IV. CONCLUSIONS

Very few analyses have been done taking into account the full one-loop corrections to the annihilation cross sections entering the computation of the relic density despite the fact that this observable is now measured within 3% precision. In supersymmetry, radiative corrections have

been known to be important, yet practically all analyses that constrain the parameter space of supersymmetry are performed with tree-level annihilation cross sections. Taking into account the full one-loop corrections to a plethora of processes is most probably unrealistic. On the other hand, one must incorporate, if possible simply and quickly, a parametrization of the theory error or implement the corrections through effective couplings of the neutralino, in the case of supersymmetry. This is what we have attempted in this study for two of the most important couplings of the neutralinos $\tilde{\chi}_1^0f\tilde{f}$ and $\tilde{\chi}_1^0\tilde{\chi}_1^0Z$. In order to look more precisely at the impact of each of these effective couplings we take as a testing ground a most simple process, $\tilde{\chi}_1^0\tilde{\chi}_1^0 \rightarrow \mu^+\mu^-$, and select a neutralino that is either almost pure bino or pure Higgsino. We do not strive at finding a scenario with the correct relic density since our primary task is to study the vertices and the approximations in detail. In this exploratory study, taking a final state involving gauge bosons would only confuse the issues. Nonetheless, the impact of the gauge bosons is studied. Indeed, we have shown how the construction of the effective $\tilde{\chi}_1^0\tilde{\chi}_1^0Z$ is quite different from that of the $\tilde{\chi}_1^0f\tilde{f}$. For the latter, the effective coupling involves self-energy corrections, whereas for the former the one-particle irreducible vertex correction must be added. These examples and the construction of the effective coupling already pave the way to a generalization to the effective couplings $\tilde{\chi}_1^0\tilde{\chi}_1^0h$, H , A , and $\tilde{\chi}_1^0\chi^+W$, which we will address in forthcoming publications with applications to different processes, including gauge boson final states. Even with the effective couplings we have derived, we could generalize the study of $\tilde{\chi}_1^0\tilde{\chi}_1^0 \rightarrow \mu^+\mu^-$ to cover not only pure winos, but also mixed scenarios and also heavy fermions.

TABLE II. Coefficients of the $\ln(m_f)$ (running couplings) $\ln(m_{\tilde{f}})$ (nondecoupling effects) in Δ_{eff} . (c, s) give very similar results to (u, d). Higgsino case.

	$a_{\tilde{Q}_L}$	$a_{\tilde{u}_R}$	$a_{\tilde{d}_R}$	a_f	$a_{\tilde{f}}$
e	0.003 04		0.000 366	0.003 09	-0.12%
(u, d)	0.008 61	0.000 489	0.000 122	(0.004 14, 0.001 01)	-0.15%
(t, b)	-0.0701	0.000 826	0.000 108	(0.004 14, 0.001 01)	0.13%

Our preliminary study on the simple process $\tilde{\chi}_1^0 \tilde{\chi}_1^0 \rightarrow \mu^+ \mu^-$ is already very instructive. To summarize the bino case, we can state that the effective couplings approach is a very good approximation that embodies extremely well the nondecoupling effects from heavy sfermions, irrespective of many of the parameters that are involved in the calculation, as long as one is in an almost pure bino case. The effective coupling implementation is within 2% of the full one-loop calculation. Here, this reflects essentially the correction to the $\tilde{\chi}_1^0 f \tilde{f}$ coupling. The scheme dependence from t_β is very small; this result stands for large M_1 masses as long as the neutralino is more than 90% binolike. In particular for Higgsino-like LSP in excess of 90 GeV as imposed by present limits on the chargino, the effective coupling implementation in the annihilation $\tilde{\chi}_1^0 \tilde{\chi}_1^0 \rightarrow \mu^+ \mu^-$ fails. It worsens as the mass increases due to the importance of a large box contribution corresponding to the opening up of $\tilde{\chi}_1^0 \tilde{\chi}_1^0 \rightarrow W^+ W^-$, which would in any case be the dominant process to take into account when calculating the relic density. The large Yukawa coupling of the top has a big impact on the radiative corrections and, in

particular, on the nondecoupling contribution of a very heavy stop. Although this is an example which shows, in principle, the failure of the effective approach apart from correctly reproducing the nondecoupling effect of very heavy squarks, we need further investigation on the dominant processes, in this case annihilations into W, Z , to see if these dominant processes could on the other hand be reproduced by an effective coupling approach. If the effective approach turns out to be efficient for the dominant processes, where and if the box corrections are tamed, the effective coupling could still be a good alternative for the calculation of the relic density with high precision. We leave many of these interesting issues to further analyses.

ACKNOWLEDGMENTS

We would like to thank Guillaume Chalons for many useful discussions. This work is part of the French ANR project, ToolsDMColl BLAN07-2 194882 and is supported in part by the GDRI-ACPP of the CNRS (France). G.D.L.R. was supported by la Région Rhones-Alpes. This work was supported by TRR33 “The Dark Universe.”

-
- [1] See, for example, S. Caron (ATLAS Collaboration), [arXiv:1106.1009](https://arxiv.org/abs/1106.1009); J.B.G. da Costa *et al.* (ATLAS Collaboration), *Phys. Lett. B* **701**, 186 (2011); G. Aad *et al.* (ATLAS Collaboration), *Eur. Phys. J. C* **71**, 1682 (2011); S. Chatrchyan *et al.* (CMS Collaboration), [arXiv:1107.1279](https://arxiv.org/abs/1107.1279).
- [2] For example, W. Murray, in “Higgs Searches at the LHC,” 2011 (unpublished).
- [3] N. Jarosik *et al.*, *Astrophys. J. Suppl. Ser.* **192**, 14 (2011).
- [4] B.A. Reid *et al.* (SDSS Collaboration), *Mon. Not. R. Astron. Soc.* **401**, 2148 (2010).
- [5] A.G. Riess *et al.*, *Astrophys. J.* **699**, 539 (2009).
- [6] E. Komatsu *et al.* (WMAP Collaboration), *Astrophys. J. Suppl. Ser.* **192**, 18 (2011).
- [7] G. Bélanger, F. Boudjema, A. Pukhov, and A. Semenov, *Comput. Phys. Commun.* **149**, 103 (2002); G. Bélanger, F. Boudjema, A. Pukhov, and A. Semenov, *Comput. Phys. Commun.* **176**, 367 (2007); G. Bélanger, F. Boudjema, A. Pukhov, and A. Semenov, *Comput. Phys. Commun.* **174**, 577 (2006); MicrOMEGAS, <http://lappth.in2p3.fr/micromegas>.
- [8] DarkSUSY: P. Gondolo *et al.*, *J. Cosmol. Astropart. Phys.* **07** (2004) 008; DarkSUSY, <http://www.physto.se/~edsjo/darksusy/>.
- [9] SuperIso Relic: A. Arbey, F. Mahmoudi, A. Arbey, and F. Mahmoudi, *Comput. Phys. Commun.* **181**, 1277 (2010); *Comput. Phys. Commun.* **182**, 1582 (2011); F. Mahmoudi, SuperISO, <http://superiso.in2p3.fr/relic/>.
- [10] N. Baro, F. Boudjema, and A. Semenov, *Phys. Lett. B* **660**, 550 (2008).
- [11] A. Freitas, *Phys. Lett. B* **652**, 280 (2007).
- [12] B. Herrmann and M. Klasen, *Phys. Rev. D* **76**, 117704 (2007); [arXiv:0709.2232](https://arxiv.org/abs/0709.2232); B. Herrmann, M. Klasen, and K. Kovarik, *Phys. Rev. D* **79**, 061701 (2009); **80**, 085025 (2009).
- [13] N. Baro, F. Boudjema, G. Chalons, and S. Hao, *Phys. Rev. D* **81**, 015005 (2010).
- [14] For a recent review, see B. Herrmann, *Proc. Sci., IDM2010* (2010) 1 [[arXiv:1011.6550](https://arxiv.org/abs/1011.6550)].
- [15] F. Boudjema, J. Edsjo, and P. Gondolo, in *Particle Dark Matter*, edited by G. Bertone (Oxford University, New York, 2010), p. 325.
- [16] H.C. Cheng, J.L. Feng, and N. Polonsky, *Phys. Rev. D* **56**, 6875 (1997); **57**, 152 (1998).
- [17] E. Katz, L. Randall, and S.f. Su, *Nucl. Phys.* **B536**, 3 (1998).
- [18] S. Kiyoura, M.M. Nojiri, D.M. Pierce, and Y. Yamada, *Phys. Rev. D* **58**, 075002 (1998).
- [19] For a recent review, see A. Hryczuk, *Phys. Lett. B* **699**, 271 (2011).
- [20] L.J. Hall, R. Rattazzi, and U. Sarid, *Phys. Rev. D* **50**, 7048 (1994); M.S. Carena, M. Olechowski, S. Pokorski, and C.E.M. Wagner, *Nucl. Phys.* **B426**, 269 (1994); M.S. Carena, D. Garcia, U. Nierste, and C.E.M. Wagner, *Nucl. Phys.* **B577**, 88 (2000).
- [21] P. Salati, *Phys. Lett. B* **571**, 121 (2003); S. Profumo and P. Ullio, *J. Cosmol. Astropart. Phys.* **11** (2003) 006; F. Rosati, *Phys. Lett. B* **570**, 5 (2003); C. Pallis, *J. Cosmol. Astropart. Phys.* **10** (2005) 015; G.B. Gelmini and P. Gondolo, *Phys. Rev. D* **74**, 023510 (2006); D.J.H. Chung, L.L. Everett, K. Kong, and K.T. Matchev, [arXiv:0706.2375](https://arxiv.org/abs/0706.2375); M. Drees, H. Imminiyaz, and M. Kakizaki, *Phys. Rev. D* **76**, 103524 (2007); A. Arbey and F. Mahmoudi, *J. High Energy Phys.* **05** (2010) 051.

- [22] A. Semenov, arXiv:hep-ph/9608488; Nucl. Instrum. Methods Phys. Res., Sect. A **389**, 293 (1997); Comput. Phys. Commun. **115**, 124 (1998); arXiv:hep-ph/0208011; Comput. Phys. Commun. **180**, 431 (2009).
- [23] J. Küblbeck, M. Böhm, and A. Denner, Comput. Phys. Commun. **60**, 165 (1990); H. Eck and J. Küblbeck, "Guide to FeynArts 1.0," Würzburg 1991 (unpublished); H. Eck, "Guide to FeynArts 2.0," Würzburg 1995 (unpublished); T. Hahn, Comput. Phys. Commun. **140**, 418 (2001).
- [24] T. Hahn and M. Perez-Victoria, Comput. Phys. Commun. **118**, 153 (1999); T. Hahn, Nucl. Phys. B, Proc. Suppl. **135**, 333 (2004); arXiv:hep-ph/0506201.
- [25] T. Hahn, LoopTools, <http://www.feynarts.de/looptools/>.
- [26] F. Boudjema, A. Semenov, and D. Temes, Phys. Rev. D **72**, 055024 (2005).
- [27] N. Baro, F. Boudjema, and A. Semenov, Phys. Rev. D **78**, 115003 (2008).
- [28] N. Baro and F. Boudjema, Phys. Rev. D **80**, 076010 (2009).
- [29] G. Bélanger, F. Boudjema, J. Fujimoto, T. Ishikawa, T. Kaneko, K. Kato, and Y. Shimizu, Phys. Rep. **430**, 117 (2006).
- [30] G. Bélanger, F. Boudjema, J. Fujimoto, T. Ishikawa, T. Kaneko, K. Kato, and Y. Shimizu, Phys. Lett. B **559**, 252 (2003).
- [31] A. Dabelstein, Z. Phys. C **67**, 495 (1995).
- [32] P. H. Chankowski, S. Pokorski, and J. Rosiek, Nucl. Phys. **B423**, 437 (1994).
- [33] D. Z. Freedman, K. Johnson, and J. I. Latorre, Nucl. Phys. **B371**, 353 (1992); P. E. Haagensen, Mod. Phys. Lett. A **7**, 893 (1992); F. del Aguila, A. Culatti, R. Muñoz Tapia, and M. Pérez-Victoria, Phys. Lett. B **419**, 263 (1998); F. del Aguila, A. Culatti, R. Muñoz Tapia, and M. Pérez-Victoria, Nucl. Phys. **B537**, 561 (1999); F. del Aguila, A. Culatti, R. Muñoz Tapia, and M. Pérez-Victoria, Nucl. Phys. **B504**, 532 (1997).
- [34] J. Guasch, W. Hollik, and J. Sola, J. High Energy Phys. **10** (2002) 040.